DISSOLUTION OF CELLULOSE WITH PYRIDINIUM-BASED IONIC LIQUIDS: EFFECT OF CHEMICAL STRUCTURE AND INTERACTION MECHANISM

ELENA S. SASHINA, DMITRII A. KASHIRSKII and KONSTANTIN N. BUSYGIN

Institute of Applied Chemistry and Ecology,
St. Petersburg State University of Industrial Technologies and Design, 18, Bol'shaya Morskaya Str., St. Petersburg, 191186, Russia
✉ *Corresponding author: Elena S. Sashina, organika@sutd.ru*

Received October 10, 2014

The results of theoretical and experimental studies of 1-alkyl-3-methylpyridinium cation-based ionic liquids (ILs) and their solutions with cellulose are presented. The obtained results show a correlation between the chemical structure of the ILs and their ability to dissolve cellulose. The mechanism of natural polymer solvation in these solvents is discussed. Our results allow us to conclude that pyridinium-based ILs are extremely promising for biomass processing. These results can help design solvents with required physical and chemical properties.

Keywords: solvents, pyridinium salts, cellulose, ionic liquid

INTRODUCTION

In recent decades, ionic liquids (ILs) have received great attention in various fields of chemistry and technology due to their unique properties. Their thermal stability, ability to be regenerated from solutions and the possibility to control their physical and chemical properties by numerous combinations of the cation-anion pair have particular importance in industrial processes.

Swatloski *et al*.[1] showed the possibility of direct cellulose dissolution in a series of different 1-alkyl-3-methylimidazolium cation-based ILs, and inspired more extensive investigations in this domain. Many investigations have been devoted to discovering new ionic liquid solvents with tuned physical and chemical properties for effective dissolution of natural polymers. This search is a complex problem since the combinations of cations and anions give a 1000 times greater number of ILs than the number of known molecular organic solvents.[2] However, not all ILs are capable to dissolve even a small amount of cellulose. It is known that solvents suitable for cellulose include nitrogenous atoms in the cations, i.e., ammonium-, imidazolium-, and pyridinium-based ILs, and anions such as $[OAc]^-$, Cl^-, Br^-, and some others.[3-11]

It has already been noticed that the application of 1,3-dialkylpyridinium-containing salts allows to obtain cellulose solutions of higher concentration in comparison with the widely studied 1,3-dialkylimidazolium-containing salts.[12-14]

Additionally, it has been reported that pyridinium-containing salts are relatively less toxic[15-17] and they decompose or mineralize faster than imidazolium salts.[18] The remaining negative effect on the environment can be minimized by the regeneration of ILs,[19-22] making the processes utilizing ILs in accordance with the principles of Green Chemistry.[23]

Pyridinium-containing ILs can become no less promising than the imidazolium-containing ILs due to their high dissolving ability and favorable ecotoxicological properties. The synthesis method of pyridinium ILs and corresponding imidazolium ILs is similar; a comparison of the cost of initial reagents shows that pyridinium-based solvents may become ca. 4 times cheaper than the most popular imidazolium ILs.

Despite the dissolving ability of pyridinium salts, which have been known since 1934,[24] there is still lack of published data on the properties of pyridinium-containing ILs. Monosubstituted pyridinium salts are also able to dissolve cellulose, however they are usually used with diluents due to their relatively high melting point.[24-25] According to Basa,[14] pyridinium salts with two substituents have lower melting points, and are better cellulose solvents. The decrease of the dissolving ability on

the positions and the number of substituents in the pyridinium ring can be represented as follows: 1,3 > 1,4 > 1,2 (see Scheme 1).

The impact of structural features on the physical-chemical properties and the dissolving ability of pyridinium-based ILs is currently poorly understood. Another important open problem is whether there is a 'structure – property' correlation in pyridinium-based ILs similar to that found in imidazolium-based ILs. Can they be similar? For imidazolium-based ILs, it has been shown that their dissolving ability is mainly determined by the nature of their anion.[25-28] Quantum chemical calculations indicate that the anion of the ionic liquids forms hydrogen bonds with hydrogen atoms of the hydroxyl groups of cellulose. At the same time, the large cation (associated with the anion) facilitates separation of neighboring cellulose macromolecules.[29-31]

NMR data and the molecular dynamics simulations generally confirm this solvation mechanism,[28,32] although some studies have suggested that the cation is also involved in hydrogen bonding with cellulose,[33-34] i.e., it is a hydrogen bond donor, while the anion is a hydrogen bond acceptor. There are data on the effect of cation acidity on the dissolution process.[20,35]

However, there is still no clear evidence of cation involvement in the hydrogen bonding with the hydroxyl groups of cellulose.[36-38] A comparison of the characteristics of the donor and acceptor properties of the ILs shows that the hydrogen-bond acceptor value (HBA) for imidazolium-based ILs determines their solubility, while the hydrogen-bond donor value (HBD) of cellulose dissolving ILs is relatively low (0.29-0.57).[39] Since the HBA is largely determined by the nature of the anion, this confirms its important role in the solvation of natural polymers by the solvent.[39] In general, imidazolium-based ILs with $\beta \geq 0.65$ may potentially dissolve cellulose, but the best dissolving ILs have $\beta \geq 0.80$.

Different types of dyes can be used in order to find the HBA and HBD parameters. One of the dyes commonly used for determining the hydrogen bond basicity is a chelate complex with the copper ion, [Cu(tmen)(acac)](ClO_4), where acac = acetylacetonate, tmen = N,N,N',N'-tetramethylethylenediamine). Since this dye is very sensitive to nucleophilic attack by the solvent, we have applied it in our work.

By confirming the application of the 'structure – property' correlation of imidazolium-based ILs for other ILs, we provide a method for the target selection of ionic solvents for cellulose, and other biopolymers.

The goal of our paper is to study the mechanism of solvation, structural features and dissolving abilities of a series of 1,3-dialkylpyridinium salts with different anions, and substituents on the cation. These data allow us to determine the notable trends of several types of ILs, and propose a mechanism of IL interaction with cellulose. Finally, our aim is to design solvents with special physical-chemical properties, which are required for green processing of natural polymers.

EXPERIMENTAL

Chemicals and reagents

For ILs: 1-butyl-3-methylimidazolium chloride (Fluka > 95%), 1-alkyl-3-methylpyridinium cation-based ILs were prepared by the alkylation reaction of 3-methylpyridine, as already described.[12]

The ionic liquids were characterized using Fourier transform infrared (FTIR) spectroscopy, nuclear magnetic resonance (^{1}H-NMR), and mass spectroscopy (MS). A brief characterization of ILs is presented in Table 1.

For the synthesis of the dye: acetylacetone (Aldrich, 99.5%), ammonia (Reakhim), N,N,N',N'-tetramethylethylenediamine (Reanal), and copper(*II*) perchlorate hexahydrate, which was obtained by reacting chloric acid and copper carbonate $CuCO_3 \cdot Cu(OH)_2$ followed by recrystallization, were used.

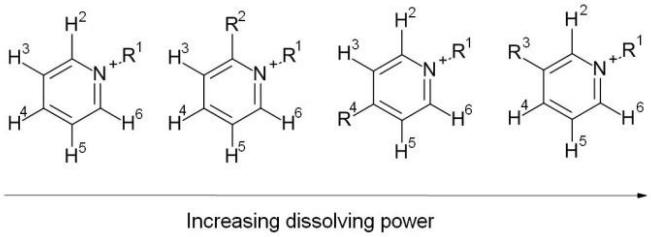

Scheme 1: Effect of position and number of alkyl substituents (R) in pyridinium cation-based ILs on their cellulose dissolving power

Table 1
Investigated ILs: structure, names and name abbreviations

Structure	Name	Abbreviation
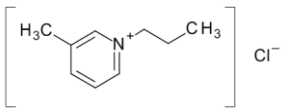	1-Propyl-3-methylpyridinium chloride	$[C_3MPy]Cl$
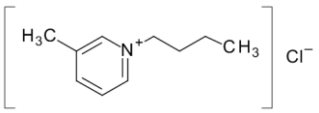	1-Butyl-3-methylpyridinium chloride	$[C_4MPy]Cl$
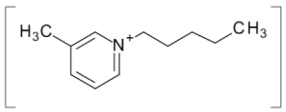	1-Pentyl-3-methylpyridinium chloride	$[C_5MPy]Cl$
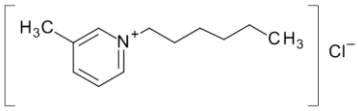	1-Hexyl-3-methylpyridinium chloride	$[C_6MPy]Cl$
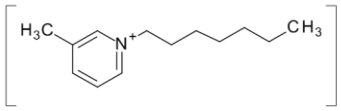	1-Heptyl-3-methylpyridinium chloride	$[C_7MPy]Cl$
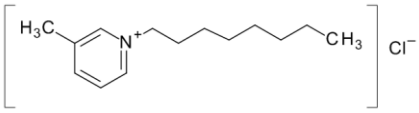	1-Octyl-3-methylpyridinium chloride	$[C_8MPy]Cl$
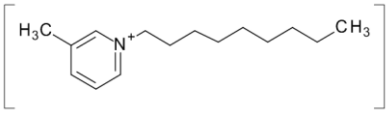	1-Nonyl-3-methylpyridinium chloride	$[C_9MPy]Cl$
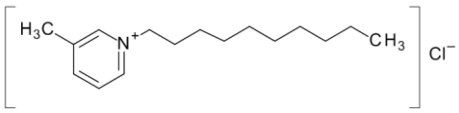	1-Decyl-3-methylpyridinium chloride	$[C_{10}MPy]Cl$
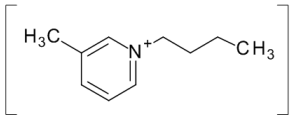	1-Butyl-3-methylpyridinium bromide	$[C_4MPy]Br$
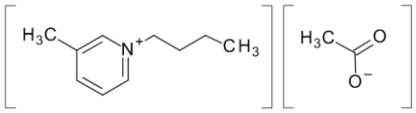	1-Butyl-3-methylpyridinium acetate	$[C_4MPy][OAc]$
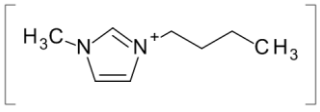	1-Butyl-3-methylimidazolium chloride	$[C_4MIm]Cl$

Synthesis of $[Cu(tmen)(acac)](ClO_4)$

The dye $[Cu(tmen)(acac)](ClO_4)$ was synthesized using the synthetic method for similar compounds,[40-42] as shown in Scheme 2.

To 10 ml of an ethanolic solution of copper (*II*) perchlorate hexahydrate (3 mmol), 10 ml of an ethanolic solution of acetylacetone (3 mmol) and ammonia (3 mmol) was added. After 30 min, 10 ml of an ethanolic solution of N,N,N',N'-tetramethylethylenediamine (3 mmol) was added. The mixture was stirred at room temperature and after 3 hours diethyl ether was added, whereupon purple crystals began to precipitate. The product was filtered and recrystallized from chloroform and diethyl ether. Then it was dried in a desiccator with P_2O_5. Yield: 73%.

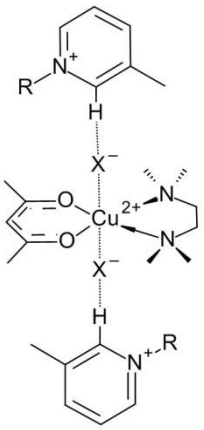

Scheme 2: Synthesis of [Cu(tmen)(acac)](ClO_4)

Dissolution of cellulose with ILs

Already established cellulose dissolution methods were followed.[12] High purity wood-derived chemical cellulose Alicell Super (with DP 599) was used for the preparation of solutions.

^{1}H-NMR studies of ILs and IL-cellulose solutions

^{1}H-NMR spectra of samples were recorded at 27 ºC using a Bruker Avance II Plus spectrometer at 700 MHz. TMS was used as internal standard (δ_H = 0.000 ppm). Details of the preparation of ILs and IL-cellulose solutions with $CDCl_3$ have already been published.[43] ^{1}H-NMR spectrum of cellulose solution in IL was performed using 4 wt% cellulose solution in [C_4MPy]Cl prepared by dissolution at 110 ºC. The solution sample (20 mg) was dissolved with 0.65 mL DMSO-d_6.

Kamlet-Taft parameter measurement

The measurements were performed on a Shimadzu UV-1800 spectrophotometer (resolution 0.1 nm) using a 2 mm quartz cuvette. ILs with dye solutions were prepared by the addition of an aqueous solution of the dye to the IL with consequent water evaporation at reduced pressure resulting in a dye concentration of ~30 mg per 100 ml IL. All samples were measured in a supercooled state.

Quantum chemical calculations

Quantum chemical calculations were performed by the Firefly QC package,[44] which is partially based on the GAMESS (US) source code,[45] DFT:B3LYP/6-311+G(d,p) method was used.

RESULTS AND DISCUSSION

Chemical structure of ionic liquids

By using the DFT:B3LYP/6-311+G(d,p) quantum chemical method the chemical structure of the series of pyridinium-based salts was investigated: 1-alkyl-3-methylpyridinium chlorides [C_nMPy]Cl (where n = 2 – 10), 1-allyl-3-methylpyridinium [AMPy]Cl,1-ethyl-3-methylpyridinium bromide [C_2MPy]Br, 1-butyl-3-methylpyridinium bromide [C_4MPy]Br, and 1-butyl-3-methylpyridinium acetate [C_4MPy][OAc]. The optimum geometry of the ionic liquids was determined by an optimization procedure, which gave the coordinates of the global minimum on the potential energy surface (PES). The potential energy of the IL's cation-anion pair formation, E_P, was calculated as a difference between the energy of the cation-anion complex, E_{CA}, and the energies of the cation, E_C, and the anion, E_A:

$$E_P = 2625.5 \cdot \{E_{CA} - (E_C + E_A)\} \quad (1)$$

where 2625.5 is the conversion factor of the Hartree energy (atomic units) in kJ mol^{-1}.

For example, the calculated PES for 1-butyl-3-methylpyridinium chloride is shown in Fig. 1. The numbering of the pyridinium ring atoms corresponds to that given in Scheme 1.

The lowest values of the potential energy E_P on the PES correspond to the two optimized structures (see Fig. 2). The global minimum with energy E_P = -364.9 kJ mol^{-1} corresponds to the position of the chloride anion, which is placed next to the H^2 proton of the cation (structure a, Fig. 2). The PES also have a similar local energy minimum for the structure with energy E_P = -360.6 kJ mol^{-1}; in this structure the anion is located close to the atom H^6 of the cation (structure b, Fig. 2).

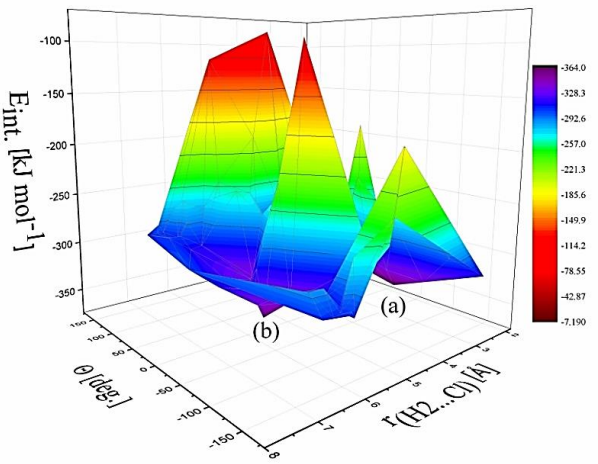

Figure 1: Dependence of the potential energy of the IL cation-anion pair formation, E_P, on the distance between the cation and anion $r_{(H2\ldots Cl)}$ and the torsion angle Θ between atoms Cl, H^2, C^2, N

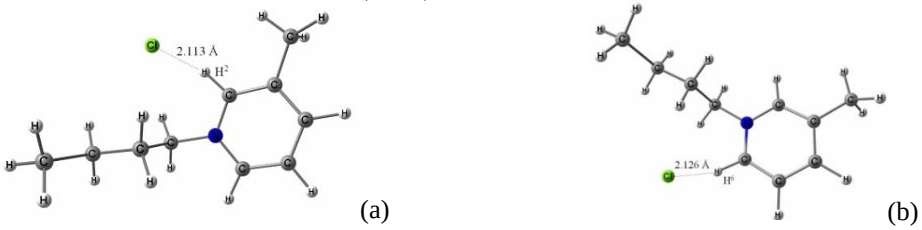

Figure 2: Two optimized structures of $[C_4MPy]Cl$ with their optimal energy, E_P values

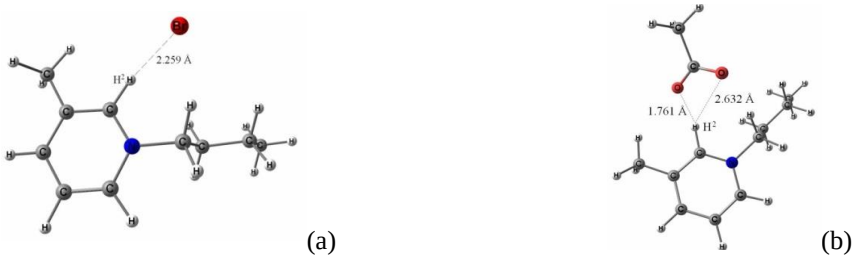

Figure 3: Optimized structures of $[C_4MPy]Br$ (a) and $[C_4MPy][OAc]$ (b)

Experimental studies by ^{1}H-NMR confirm that the atoms H^2 and H^6 in the pyridinium ring are the most sensitive to the proximity of the anion, and they have the maximal values of chemical shifts.[43] The overall global minimum (E_P) on the PES is observed for the model with the anion located close to the H^2 ring proton. This structure of $[C_nMPy]Cl$ is the most stable and therefore, this model was chosen for the further calculations.

It should be noted that the obtained values of the potential energy of the ion pairs are comparable with the results of the chemical structure calculations for imidazolium-based ILs (from -302 kJ mol^{-1} to -392 kJ mol^{-1}).[29,46] The results of the quantum chemical calculations for the 1,3-dialkylimidazolium salts are very close to those presented here for pyridinium salts: anion occupies a similar position next to the most acidic ring proton H^2, located between the two alkyl substituents of the imidazolium ring. This corresponds to the most energetically favorable location of the anion around the cation.[29,47-48]

The data of the ^{1}H-NMR spectroscopy confirm the results.[10,49]

Our results of quantum chemical calculations for all studied pyridinium ILs showed the chemical structure with a similar location of anions around cations. The optimized models, for example $[C_4MPy]Br$ and $[C_4MPy][OAc]$, are shown in Fig. 3.

The main results of the quantum chemical calculations are shown in Table 2. The locations of cations around anions can be characterized by a torsion angle, Θ, between anion X and the following pyridinium ring atoms: H^2, C^2, and N, and by distance ($r_{(H2\ldots X)}$) between anion X and the nearest atom H^2 of the cation. We see that the chloride anions, for 1-alkyl-3-methylpyridinium chloride-based ILs, are located close to the plane of pyridinium rings. In this case, the torsion angle ranges from 20º to 30º, and it deviates with the elongation of the alkyl substituent.

For the studied bromide-based IL models, the torsion angles have larger values. In this case, the anions are located out of the plane of pyridinium rings. The Θ angle for 1-allyl-3-methylpyridinium chloride has the opposite sign values, because the cation is located on the other side of the plane of the ring.

A similar characteristic for 1-butyl-3-methylimidazolium halide-based ILs was found earlier:[50] the angle N1 – C2 – H – X (indicated as Θ in our work), and the distance between the cation and anion are increasing in the series $Cl^- < Br^- < I^-$.

We also observed that with the elongation of the alkyl chains the distances between the cation and anion $r_{(H2\ldots X)}$ increased from 2.056 Å in $[C_2MPy]Cl$ to 2.112 Å in $[C_{10}MPy]Cl$. This is confirmed by ^{1}H-NMR. In the homologous series, we observed a decrease of the chemical shift values, δ, for protons H^2 and H^6. These protons have the greatest sensitivity with respect to the location of the anions, see Fig. 4. A chemical shift of the ring proton signal downfield means that the distance between the electronegative anions and the cations increases.[43]

Since we observe increasing torsion angle values between the anion and the cation in the homologous series, we can conclude that ion coupling weakened and cation-anion pairs became less associated. The data presented in Table 2 show that there is a decrease in the potential energy of the IL's cation-anion pair formation (E_P) in the homologous series. As a result, the decrease of the packing density of the ions in the crystal leads to a reduction of the IL's melting point.[51] A similar behavior is observed for the imidazolium salts: a correlation is noticeable when the calculated inter-ion distance values of 1-alkyl-3-methylimidazolium chloride-based ILs[36] and melting points of these salts are compared.[52]

Table 2
Selected physical and chemical parameters calculated by DFT:B3LYP/6-311+G(d,p) for the series of pyridinium-based ILs under study

IL models	$r_{(H2\ldots X)}$, Å	Θ, deg.	$q_{(X)}$	$q_{(C)}$	μ, D	E_P, kJ mol^{-1}
$[C_2MPy]Cl$	2.056	-19.0	-0.698	0.698	13.19	-400.7
$[C_3MPy]Cl$	2.110	-23.1	-0.707	0.707	13.11	-366.1
$[C_4MPy]Cl$	2.113	-18.2	-0.708	0.708	12.98	-364.9
$[C_5MPy]Cl$	2.112	-26.0	-0.707	0.707	12.91	-364.0
$[C_6MPy]Cl$	2.111	-23.3	-0.708	0.708	12.86	-363.6
$[C_7MPy]Cl$	2.111	-23.3	-0.708	0.708	12.87	-363.2
$[C_8MPy]Cl$	2.115	-30.0	-0.709	0.709	12.79	-362.8
$[C_9MPy]Cl$	2.113	-28.0	-0.709	0.709	12.67	-362.9
$[C_{10}MPy]Cl$	2.112	-23.1	-0.708	0.708	12.80	-362.5
[AMPy]Cl	2.096	15.6	-0.692	0.692	13.32	-413.8
$[C_2MPy]Br$	2.238	-32.3	-0.660	0.660	13.80	-378.9
$[C_4MPy]Br$	2.259	-29.0	-0.644	0.644	13.44	-369.9
$[C_4MPy][OAc]$	1.761, 2.632[A]		-0.808	0.808	10.42	-394.0

[A]Distances between atom H^2 of cation and two oxygen atoms of acetate anion

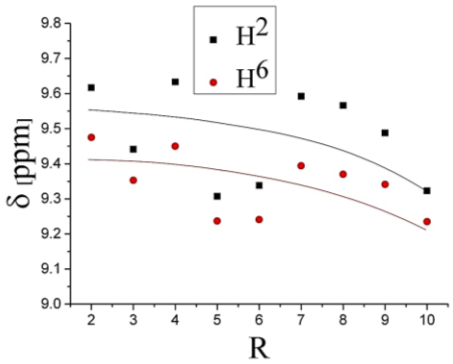

Figure 4: ^{1}H-NMR chemical shift values of the pyridinium ring H^2 and H^6 protons for 1-alkyl-3-methylpyridinium chloride-based ILs with increased alkyl chain length (R).
Chemical shifts are obtained in $CDCl_3$

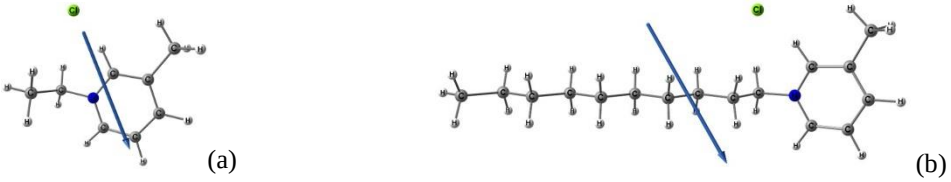

(a) (b)

Figure 5: Displacement of the vector of the dipole moments for [C_2MPy]Cl (a) and [C_{10}MPy]Cl (b)

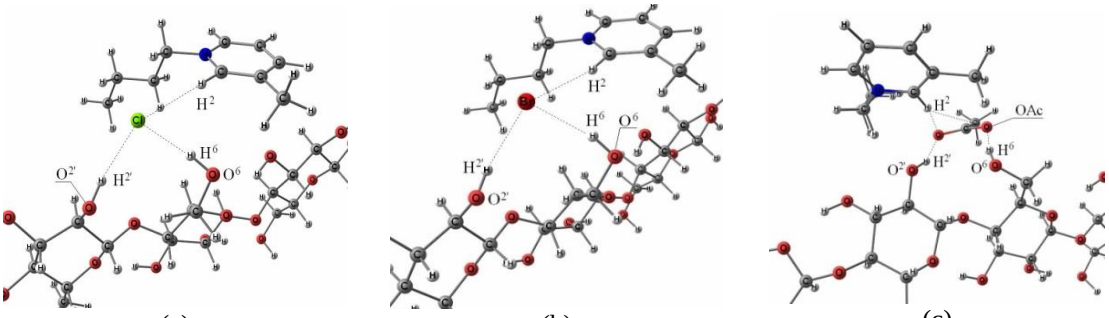

(a) (b) (c)

Figure 6: Optimized solvate complexes of cellotetraoses with 1-butyl-3-methylpyridinium chloride (a), 1-butyl-3-methylpyridinium bromide (b), and 1-butyl-3-methylpyridinium acetate (c)

Table 3
Main calculated parameters for the solvated complexes of cellotetraose with [C_4MPy][OAc], [C_4MPy]Cl and [C_4MPy]Br

ILs	$r_{(H2\ldots X)}$, Å	Φ_2, deg.	Φ_6, deg.	$r_{(O2'H2'-X)}$, Å	$r_{(O6H6-X)}$, Å
[C_4MPy][OAc]	2.080, 2.750[A]	157.56	168.58	1.716	1.737
[C_4MPy]Cl	2.485	167.18	168.50	2.327	2.129
[C_4MPy]Br	2.605	167.16	160.16	2.650	2.374

Φ_2 – Angle between cellotetraose atoms $O^{2'}$, $H^{2'}$, and the anion X;
Φ_6 – Angle between cellotetraose atoms O^6, H^6, and the anion X;
[A]Distances between atom H^2 of cation and two oxygen atoms of acetate anion

Increasing the substituent carbon chain lengths does not lead to significant changes in the charges of the cation, $q_{(C)}$, for halide-containing ILs. However, such an increase leads to a decrease in the solvent polarity as a result of increasing the volume portion of non-polar components. The electric dipole moment μ values, which are characteristic of the electron density asymmetry, are gradually reduced in chloride-containing ILs, where the length of the substituents is increased. The displacement of the vector of the dipole moment along the alkyl chain takes place gradually, as shown in Fig. 5. The calculated values of μ for bromide-containing ILs also decrease as the alkyl chain length of cation substituent increases.

Interaction of ionic liquids with cellulose

Quantum chemical calculations of the solvated complexes of cellulose and 1-butyl-3-methylpyridinium-based ILs containing chloride-, bromide-, and acetate-anions were performed. Cellotetraose is used as a model compound of cellulose (a cellulose polysaccharide fragment consisting of four glycosidic residues). Optimal complexes of cellotetraoses with 1-butyl-3-methylpyridinium chloride, 1-butyl-3-methylpyridinium bromide and 1-butyl-3-methylpyridinium acetate are shown in Fig. 6, and Table 3 summarizes their calculated structural parameters.

The interaction in the studied complexes is accompanied by the formation of two hydrogen bonds between the anion of the IL and the primary hydroxyl group, and the anion and the neighboring secondary hydroxyl group of the cellotetraose. Similar solvate complexes with energy of 80 kJ mol^{-1} or higher are also formed by using the other direct cellulose solvents. These solvents have strong electron donor sites, such as the oxygen atom of N-methylmorpholine-N-oxide (NMMO), or the anion of imidazolium-based ILs, which are able to form two hydrogen bonds with the neighboring cellulose hydroxyls.[29-30,53-55] It should be noted that the electron acceptor site of solvents (the nitrogen atom of NMMO, and the cation of IL) cannot form hydrogen bonds with the hydroxyl groups of cellulose.

To quantify and characterize the solvate complexes of 'cellotetraose – 1-butyl-3-methylpyridinium-based ILs, we noted the following: (1) distances between the anion and the hydrogen atoms of the cellotetraose hydroxyls ($r_{(O6H6\text{-}X)}$ and $r_{(O2'H2'\text{-}X)}$) lie in the interval between 1.7 Å and 2.7 Å, and valence angles are 157.6-168.6º. These distances increase in the series $[C_4MPy][OAc]$ < $[C_4MPy]Cl$ < $[C_4MPy]Br$. The obtained geometric characteristics satisfy the required criteria for hydrogen bond formation. For example, the distance C_{sp^3}–$OH\cdots Cl^-$ at hydrogen bond formation with chloride-anion is between ~2 and ~2.4 Å, and the valence angle Φ (between atoms O, H and Cl) > 140º.[56] (2) The anion of the solvent is located closer to the hydrogen atom of the primary hydroxyl group O^6H^6. The molecular dynamics calculations for the cellulose interaction with imidazolium-based IL $[C_4MIm]Cl$ showed similar results:[28] on average, primary OH groups interact more intensively with the chloride-anion in comparison with the secondary OH groups. The interaction of both hydroxyls with the anion is within the range of distances between 2.3 Å and 4 Å.

The interactions of $[C_4MPy]Br$ with cellotetraose (see Fig. 6(b)), as shown by quantum chemical calculations, are similar: the anion form hydrogen bonds both with the primary and secondary cellotetraose hydroxyls. The distances between bromide-anions and cellotetraose hydroxyls are longer than in the case of chloride-anions (2.374 Å for O^6H^6...Br, and 2.650 Å for $O^{2'}H^{2'}$...Br). This seems reasonable if we take into account that the hydrogen bond lengths between halides and H-donors increase at larger halide ion volumes.[56] Since the hydrogen bond length indirectly characterizes the interaction energy, it is quite understandable that $[C_4MPy]Br$ dissolves cellulose much more poorly than $[C_4MPy]Cl$.[12]

The obtained results on the distances between interacting atoms allow us to calculate the hydrogen bond energies for solvated complexes of cellotetraose with $[C_4MPy][OAc]$. This can be performed by the following formula:[57]

$$E_{HB(H\ldots O)} = \frac{A'_{H\ldots O}}{r_{(H\ldots O)}{}^{12}} - \frac{B_{H\ldots O}}{r_{(H\ldots O)}{}^{10}} \qquad (2)$$

where $A'_{H\ldots O}$ and $B_{H\ldots O}$ are specific coefficients for different combinations of hydrogen-bonding H and O atoms. The values of these coefficients for a suitable chemical (i.e. acetic acid) are 13344 kkal/Å^{12} mol, and 5783 kkal/Å^{10} mol, respectively.[58] The energy value is obtained by using the conversion factor 1 kkal = 4.1868 kJ. Thus, the hydrogen bonds energies between the oxygen atoms of acetate-anion and hydrogen atoms of cellotetraose hydroxyls, $E_{HB(O\ldots H)}$, have values of -23.7 kJ per $O\cdots H^{2'}$ hydrogen bond, and of -22.8 kJ per the $O\cdots H^6$ hydrogen bond. To our knowledge, there are no published data on the calculations of the hydrogen bond energies with cellulose for other ILs.

The formation of the solvate complex between the solvent and cellotetraose is accompanied by an increase in the distance between the solvent's anion and cation $r_{(H2\ldots X)}$ with the following values: 0.319 (and 0.118) Å for acetate, 0.372 Å for chloride, and 0.346 Å for bromide. Therefore, the ionic bond between the cation and anion has a tendency to be weakened, and this fact is confirmed by the results of ^{1}H-NMR studies.[43] This effect is presented in Fig. 7, where the chemical shifts for pyridinium ring protons H^2 ($\Delta\delta_{H2}$ = -0.060 ppm) and H^6 ($\Delta\delta_{H6}$ = -0.025 ppm) peaks can be observed, while the chemical shifts for H^4 and H^5 atoms are almost unchanged ($\Delta\delta_{H4,H5}$ = 0.007-0.009 ppm). This decrease occurred due to the reduced influence of the receding anion. Earlier it was noted that the anion was most likely associated with the cation by the atom H^2 and, to a lesser extent, by the atom H^6 of 1,3-disubstituted pyridinium ring atoms which these studies support.

The interaction of the anion with the secondary hydroxyls of cellulose glycosidic cycles is confirmed by ^{1}H-NMR (see Fig. 8). To explain the peaks for cellulose, we have used the data from the work of Bernet and Vasella,[59] where the chemical shifts of the disaccharide (cellobiose) were investigated. The chemical shifts of the hydrogen atoms in the secondary hydroxyls have the values for cellobiose of δ_{O2H2} = 4.630 ppm, $\delta_{O2'H2'}$ = 5.215 ppm, were moved downfield ($\Delta\delta_{O2'H2'}$ = 0.171 ppm, $\Delta\delta_{O2H2}$ = 0.067 ppm) when solvated by $[C_4MPy]Cl$. This effect is the result of the interaction of cellulose with the chloride-anion. Thus, the intramolecular hydrogen bond in the structure of cellulose is broken when cellulose is dissolved in the IL. The hydrogen atom of the secondary OH-group forms the $O^{2'}H^{2'}\cdots Cl^-$ hydrogen bond with the anion. It is difficult to estimate the level of interaction of the anion with the primary hydroxyls by this method since the peaks of the primary hydroxyls of the C^6 (and $C^{6'}$) atom overlap with other peaks, including the peak of the methylene group CH_2 (1') from the alkyl chain on the cation of $[C_4MPy]Cl$.

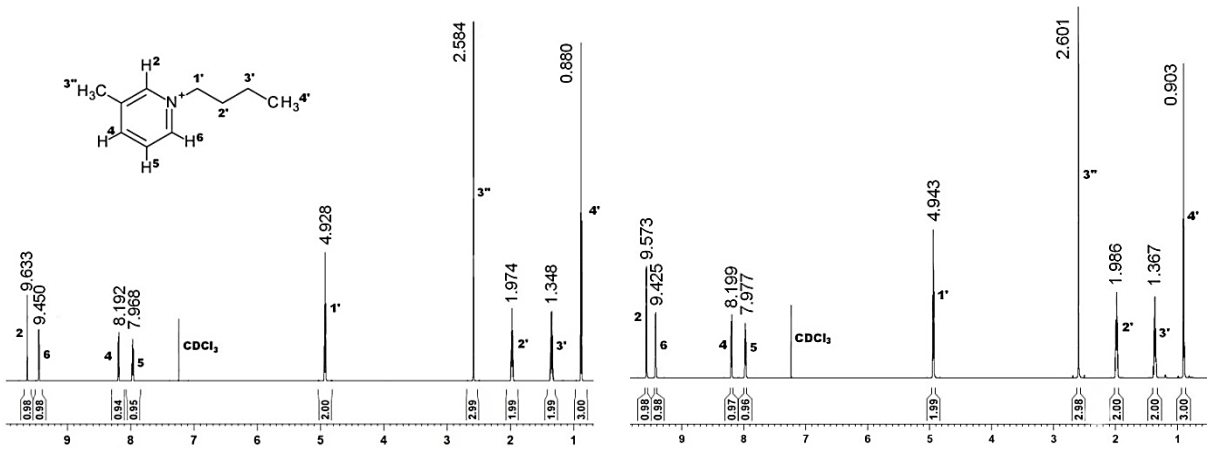

(a) (b)

Figure 7: ^{1}H-NMR spectra for 1-butyl-3-methylpyridinium chloride (a), and solution of 1-butyl-3-methylpyridinium chloride with cellulose (b). ^{1}H-NMR spectra were obtained in $CDCl_3$

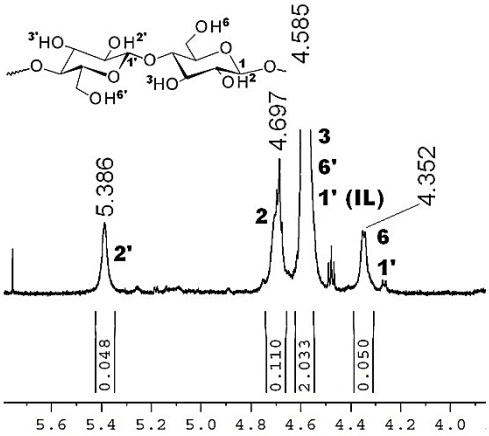

Figure 8: Partial ^{1}H-NMR spectrum for cellulose in solution with 1-butyl-3-methylpyridinium chloride. ^{1}H-NMR spectrum was obtained in DMSO-d_6

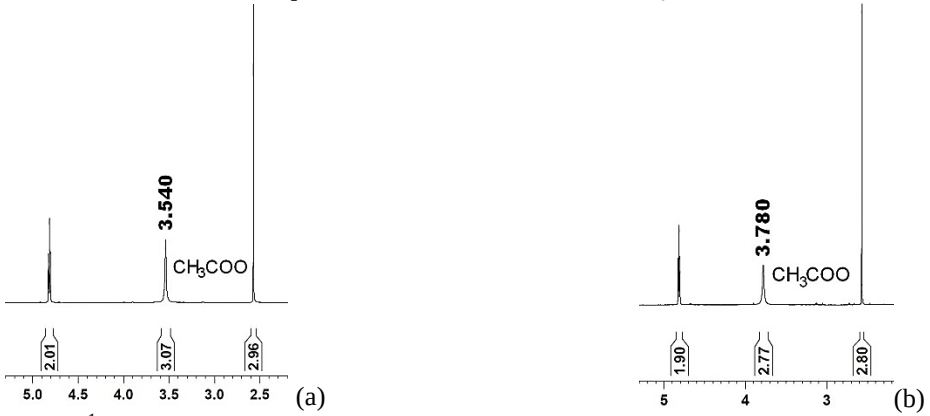

(a) (b)

Figure 9: Partial ^{1}H-NMR spectrum for 1-butyl-3-methylpyridinium acetate (a), and solution of 1-butyl-3-methylpyridinium acetate with cellulose (b). ^{1}H-NMR spectra were obtained in $CDCl_3$

According to the quantum chemical calculations, the interaction of 1-butyl-3-methylpyridinium acetate with cellotetraose leads to the displacement of the anion with respect to the plane of the pyridinium ring. Moreover, one closest oxygen atom of the anion moves slightly away from the cation, while the other oxygen atom comes closer to the cation. This behavior can be explained by the reorientation of acetate-anion in space, so that it can form hydrogen bonds with the cellotetraose hydroxyls. The movement of the anion can also be traced by interpreting the ^{1}H-NMR data: the chemical shift of the CH_3-group protons of the anion is significantly displaced downfield (see Fig. 9).

This strong deshielding can be explained by distancing of the oxygen atoms during the hydrogen bond formation with cellotetraose.

When our experimental results are compared to the published data of ^{1}H-NMR spectra of the solutions of cellulose in 1-butyl-3-methylimidazolium-based ILs, it becomes clear that the signals of hydroxylic hydrogen atoms of the cellulose dissolved in 1-butyl-3-methylpyridinium ILs are shifted downfield.[33] At the same time, the imidazolium ring protons are shifted upfield:[33,42] the presence of cellulose in the solution strongly affects the most acidic hydrogen atoms ($H^2 > H^4 > H^5$). For cellulose solutions in 1-butyl-3-methylimidazolium acetate the ring protons are shifted upfield by 0.10-0.17 ppm.[60] This effect may indicate an increasing distance between the anion and the cation (in this case, the cation does not form hydrogen bonds with cellulose). This shift is larger in magnitude than the shifts obtained in this work, due to the difference of cations and anions from various ILs, and the difference of solution concentrations. Generally, the experimental and calculated data for mechanisms of cellulose dissolving in imidazolium- and pyridinium-based ILs are very similar.

Overall, the quantum chemical calculations results and ^{1}H-NMR chemical shifts data show that the interaction of cellulose with pyridinium-containing ILs is possible due to the ability of the anion to be hydrogen bond acceptor.

Ionic liquids basicity (β)

To find the Kamlet-Taft hydrogen bond basicity parameter (β) for 1-alkyl-3-methylpyridinium-based ILs, the dye [Cu(tmen)(acac)](ClO_4) can be used, which is very sensitive to nucleophilic attack by the solvent.[61] The following equation allows to find the parameter β from its UV spectra in IL:[62]

$$\beta = \frac{\tilde{\nu}_{max} - \tilde{\nu}_0}{b} \qquad (3)$$

where $\tilde{\nu}_0$ = 18.82 kK is values of the wavenumbers corresponding to the neat dye and b = 2.71. The value of $\tilde{\nu}_{max}$ is the peak of maximum absorption in the spectrum of the dye solution in the studied ILs in kK (1 kiloKayser = 1000 cm^{-1}).

The [Cu(tmen)(acac)](ClO_4) chelate complex has unequal strength of axial and equatorial ligands.[63-64] In solution only the axial ligands are solvated. In ionic liquids perchlorate-anions tend to be substituted, as shown in Scheme 3.

Table 4 summarizes the results of the spectrophotometric data of the β values (hydrogen bond acceptor) for pyridinium-based ILs. To confirm the reliability of this spectrophotometric method, an investigation of the solution of 1-butyl-3-methylimidazolium chloride [C_4MIm]Cl was also performed.

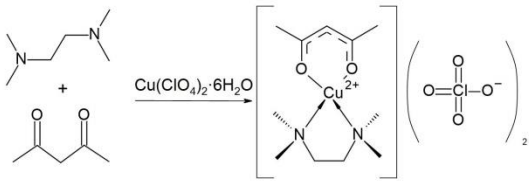

Scheme 3: Solvation of [Cu(tmen)(acac)](ClO_4) by 1-alkyl-3-methylpyridinium-based ILs

Table 4

Spectral characteristics of solutions of [Cu(tmen)(acac)](ClO_4) with 1-alkyl-3-methylpyridinium-based ILs and [C_4MIm]Cl, and the concentration of dissolved cellulose Alicell Super (DP 599) at 110 ºC in selected ILs (*D*)

№	ILs	$\tilde{\nu}_{max}$, kK	β	*D*, wt%,[12]
1	[C_3MPy]Cl	21.501	0.99	22
2	[C_5MPy]Cl	21.313	0.92	21
3	[C_6MPy]Cl	20.978	0.80	19
4	[C_7MPy]Cl	21.026	0.82	14.5
5	[C_8MPy]Cl	20.881	0.76	6.5
6	[C_9MPy]Cl	20.921	0.78	4
7	[C_{10}MPy]Cl	20.790	0.73	6
8	[C_4MPy]Br	20.717	0.70	3.4
9	[C_4MIm]Cl	21.404	0.95	17

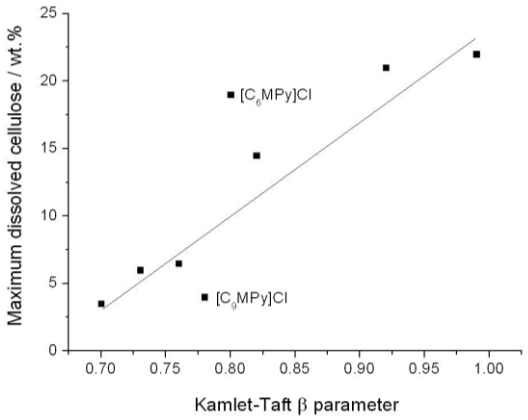

Figure 10: Correlation between the Kamlet-Taft β parameter values and the dissolving power of 1-alkyl-3-methylpyridinium-based ILs

The β parameters of the studied ILs are sufficiently large. Their maximum value (0.99) is larger than that of 1-butyl-3-methylimidazolium chloride (0.95), which is an indication of a high cellulose dissolution ability (β value was obtained using the same dye). It was found that HBA depends not only on the nature of the anion, but also on the alkyl chain length of the cation. Table 4 shows that the elongation of the alkyl chain on the 1-alkyl-3-methylpyridinium cation and the substitution of the chloride-anion for the bromide-anion decrease the basicity parameter of solvents. From Fig. 10, we see that, in general, the parameter β values are well correlated with the cellulose dissolution abilities of 1-alky-3-methylpyridinium-based ionic liquids (maximum cellulose concentrations are investigated elsewhere[12]). A similar correlation was observed for imidazolium-based ILs.[64-65] A decrease of the dissolution ability with respect to cellulose for imidazolium-based ILs is also observed depending on the cation structure.[66] Pyridinium-based ILs with β values higher than 0.8 are capable to dissolve cellulose. The absolute values of parameter β, for cellulose dissolving imidazolium- and pyridinium-based ILs, are very similar. This fact allows us to predict the cellulose dissolution ability of the whole range of ILs based on these cations.

CONCLUSION

We have performed a comprehensive study of the cellulose dissolution ability of a series of pyridinium-based ILs. We have identified the main characteristics of the structure, as well as the physical and chemical properties of pyridinium-based ILs affecting cellulose dissolution. Moreover, it was found that pyridinium-based ILs have similar common patterns that are typical of imidazolium-based solvents.

Optimal geometries and electron density distributions for 1-alkyl-3-methylpyridinium chlorides, bromides, and acetates ion pairs were obtained by DFT:B3LYP quantum chemical calculations. It was found that the elongation of the alkyl chain at the pyridinium cation and the change of anion from Cl^- to Br^- lead to:

(1) distancing of the anion from the cation, (2) a decrease of the interaction energy values and (3) a decrease of the dipole moment values for the ion pair (which is characterized by the asymmetry of the electron density distribution).

By quantum chemical calculations, the optimal structure of the solvate complexes of cellotetraose with 1-butyl-3-methylpyridinium chloride, bromide, and acetate was found. It was revealed that the solvation occurs through hydrogen bond formation between the IL's anion and the two neighboring cellotetraose hydroxyl groups. It should be noted that anions strongly interaction with the O^6H^6 cellotetraose hydroxyl group, but not with the $O^{2'}H^{2'}$ hydroxyl. The calculated hydrogen bonding energies for the model of cellulose with 1-butyl-3-methylpyridinium acetate give a value of -23.7 kJ per bond. The cation does not form hydrogen bonds with cellotetraose and remains associated with the anion, but the distances between the ion pairs increase.

The main calculated characteristics are confirmed, in general, by the chemical shifts of the ILs, and the IL solutions with cellulose.

The basicity (β parameter) values of the studied pyridinium-based ILs have been obtained. The β values for the ILs are quite high (up to 0.99), and they depend not only on the nature of the anion, but also on the alkyl chain length of the cation. Calculated β values decrease with increased alkyl chain length and change of Cl^- to Br^-. The HBA for pyridinium-based ILs have a good correlation with their cellulose dissolution ability.

ACKNOWLEDGEMENTS: This work was supported by the Ministry of Education and Science of the Russian Federation (State Task No. 2014/186).

REFERENCES

[1] R. P. Swatloski, S. K. Spear, J. D. Holbrey, R. D. Rogers, *J. Am. Chem. Soc.*, **124**, 4974 (2002).
[2] S. Sowmiah, V. Srinivasadesikan, M. C. Tseng, Y. H. Chu, *Molecules*, **14**, 3780 (2009).
[3] S. S. Y. Tan, D. R. MacFarlane, *Top. Cur. Chem.*, **290**, 311 (2010).
[4] A. M. Costa Lopes, K. G. Joãoa, D. F. Rubik, E. Bogel-Łukasik, L. C. Duarte *et al.*, *Bioresour. Technol.*, **142**, 198 (2013).
[5] T. Liebert, T. Heinze, *BioResources*, **3**, 576 (2008)
[6] L. J. A. Conceiçao, E. Bogel-Łukasik, R. Bogel-Łukasik, *RSC Adv.*, **2**, 1846 (2012).
[7] M. E. Zakrzewska, E. Bogel-Łukasik, R. Bogel-Łukasik, *Energ. Fuel.*, **24**, 737 (2010).
[8] E. S. Sashina, N. P. Novoselov, O. G. Kuz'mina, S. V. Troshenkova, *Fibre Chem.*, **40**, 270 (2008).
[9] O. G. Kuzmina, E. S. Sashina, N. P. Novoselov, M. Zaborski, *Fibres Text. East. Eur.*, **77**, 36 (2009**)**.
[10] S. V. Troshenkova, E. S. Sashina, N. P. Novoselov, K. F. Arndt, *Russ. J. Gen. Chem.*, **80**, 501 (2010).
[11] O. G. Kuzmina, E. S. Sashina, S. V. Troshenkowa, D. Wawro, *Fib. Text. in East. Eur.*, **80**, 32 (2010).
[12] E. S. Sashina, D. A. Kashirskii, M. Zaborski, S. Jankowski, *Russ. J. Gen. Chem.*, **82**, 1994 (2012).
[13] T. Heinze, K. Schwikal, S. Barthel, *Macromol. Biosci.*, **5**, 520 (2005).
[14] M. L. T. N. Basa, Master Thesis, University of Toledo, 2010.
[15] C. W. Cho, Y. C. Jeon, T. P. T. Pham, K. Vijayaraghavan, Y. S. Yun, *Ecotox. Environ. Saf.*, **71**, 166 (2008).
[16] D. J. Couling, R. J. Bernot, K. M. Docherty, J. N. K. Dixon, E. J. Maginn, *Green Chem.*, **8**, 82 (2006).
[17] K. M. Docherty, C. F. Kulpa, *Green Chem.*, **7**, 185 (2005).
[18] K. M. Docherty, J. N. K. Dixon, C. F. Kulpa, *Biodegradation*, **18**, 481 (2007).
[19] A. W. T. King, J. Asikkala, I. Mutikainen, P. Järvi, I. Kilpeläinen, *Angew. Chem. Int. Ed.*, **50**, 6301 (2011).
[20] A. Parviainen, A. W. T. King, I. Mutikainen, M. Hummel, C. Selg *et al.*, *Chem. Sus. Chem.*, **11**, 2161 (2013).
[21] A. J. Holding, M. Heikkilä, I. Kilpeläinen, A. W. T. King, *Chem. Sus. Chem.*, **7**, 1422 (2014).
[22] K. Shill, S. Padmanabhan, Q. Xin, J. M. Prausnitz, D. S. Clark *et al.*, *Biotechnol. Bioeng.*, **108**, 511 (2011).
[23] P. T. Anastas, J. C. Warner, "Green Chemistry: Theory and Practice", Oxford University Press, New York, USA, 1998.
[24] US Patent 1943176, 1934.
[25] N. Jiang, A. J. Ragauskas, in "Ionic Liquids: Applications and Perspectives", edited by A. Kokorin, InTech, Rijeka, Croatia, 2011, pp. 529-544.
[26] S. P. M. Ventura, C. M. S. S. Neves, M. G. Freire, I. M. Marrucho, J. Oliveira *et al.*, *J. Phys. Chem. B*, **113**, 9304 (2009).
[27] A. Brandt, J. P. Hallett, D. J. Leak, R. J. Murphy, T. Welton, *Green Chem.*, **12**, 672 (2010).
[28] Z. Liu, R. C. Remsing, P. B. Moore, G. Moyna, in *Ionic Liquids IV*, Am. Chem. Soc., 2007, vol. 975, ch. 23, pp. 253-255.
[29] E. S. Sashina, N. P. Novoselov, *Russ. J. Gen. Chem.*, **79**, 1057 (2009).
[30] N. P. Novoselov, E. S. Sashina, V. E. Petrenko, M. Zaborsky, *Fibre Chem.*, **39**, 153 (2007).
[31] B. D. Rabideau, A. Agarwal, A. E. Ismail, *J. Phys. Chem. B*, **117**, 3469 (2013).
[32] R. C. Remsing, R. P. Swatloski, R. D. Rogers, G. Moyna, *Chem. Commun.*, **278**, 1271 (2006).
[33] O. A. El Seoud, V. C. da Silva, S. Possidonio, R. Casarano, E. P. G. Areas *et al.*, *Macromol. Chem. Phys.*, **212**, 2541 (2011).
[34] L. Feng, Z. Chen, *J. Mol. Liq.*, **142**, 1 (2008).
[35] B. Lu, A. Xu, J. Wang, *Green Chem.*, **16**, 1326 (2014).
[36] J. Zhang, H. Zhang, J. Wu, J. Zhang, J. He *et al.*, *Phys. Chem. Chem. Phys.*, **12**, 1941 (2010).
[37] R. C. Remsing, I. D. Petrik, Z. Liu, G. Moyna, *Phys. Chem. Chem. Phys.*, **12**, 14827 (2010).
[38] J. Zhang, H. Zhang, J. Wu, J. Zhang, J. He *et al.*, *Phys. Chem. Chem. Phys.*, **12**, 14829 (2010).
[39] M. Gericke, P. Fardim, T. Heinze, *Molecules*, **17**, 7458 (2012).
[40] C. D. Ene, F. Tuna, O. Fabelo, C. Ruiz-Pérez, A. M. Madalan *et al.*, *Polyhedron*, **27**, 574 (2008).
[41] A. M. Madalan, V. C. Kravtsov, D. Pajic, K. Zadro, Y. A. Simonov *et al.*, *Inorg. Chim. Acta*, **357**, 4151 (2004).
[42] C. C. Su, S. P. Wu, C. Y. Wu, T. Y. Chang, *Polyhedron*, **14**, 267 (1995).

[43] E. S. Sashina, D. A. Kashirskii, S. Jankowski, *Fibre Chem*., **45**, 268 (2014).
[44] Alex A. Granovsky, Firefly version 8.0, www http://classic.chem.msu.su/gran/firefly/index.html.
[45] M. W. Schmidt, K. K. Baldridge, J. A. Boatz, S. T. Elbert, M. S. Gordon *et al*., *J. Comput. Chem*., **14**, 1347 (1993).
[46] K. Dong, S. Zhang, D. Wang, X. Yao, *J. Phys. Chem. A*, **110**, 9775 (2006).
[47] E. A. Turner, C. C. Pye, R. D. Singer, *J. Phys. Chem. A*, **107**, 2277 (2003).
[48] P. A. Hunt, B. Kirchner, T. Welton, *Chem. Eur. J*., **12**, 6762 (2006).
[49] J. G. Huddleston, A. E. Visser, W. M. Reichert, H. D. Willauer, G. A. Broker *et al*., *Green Chem*., **3**, 156 (2001).
[50] M. Shukla, N. Srivastava, S. Saha, *J. Mol. Struct*., **975**, 349 (2010).
[51] E. S. Sashina, D. A. Kashirskii, G. Janowska, M. Zaborski, *Thermochim. Acta*, **568**, 185 (2013).
[52] S. Zhang, X. Lu, Q. Zhou, X. Li, X. Zhang *et al*., "Ionic Liquids: Physicochemical Properties", Elsevier, 2009.
[53] N. P. Novoselov, E. S. Sashina, A. P. Kuznetsova, V. E. Petrenko, *Russ. J. Phys. Chem. A*, **81**, 1706 (2007).
[54] R. J. Marhöfer, K. M. Kast, B. Schilling, H. J. Bär, S. M. Kast *et al*., *Macromol. Chem. Phys*., **201**, 2003 (2000).
[55] N. P. Novoselov, E. S. Sashina, V. E. Petrenko, A. P. Kuznetsova, *Russ. J. Phys. Chem. A*, **S1**, S108 (2005).
[56] T. Steiner, *Acta Cryst.*, **B54**, 456 (1998).
[57] F. A. Momany, R. F. McGuire, A. W. Burgess, H. A. Scheraga, *J. Phys. Chem*., **79**, 2361 (1975).
[58] F. A. Momany, R. M. Carruthers, R. F. McGuire, H. A. Scheraga, *J. Phys. Chem*., **78**, 1595 (1974).
[59] B. Bernet, A. Vasella, *Helv. Chim. Acta*, **83**, 2055 (2000).
[60] O. Kuzmina, S. Jankowski, A. Fabiańska, E. Sashina, D. Wawro, *Cellulose Chem. Technol*., **48**, 45 (2014).
[61] R. W. Soukup, K. Sone, *Bull. Chem. Soc. Jpn*., **60**, 2286 (1987).
[62] Y. Marcus, Y. Migron, *J. Phys. Chem*., **95**, 400 (1991).
[63] K. Sone, Y. Fukuda, in "Inorganic Thermochromism", edited by K. Sone and Y. Fukuda, Springer-Verlag, Berlin, 1987, vol. 10, ch. D.
[64] R. W. Soukup, R. Schmid, *J. Chem. Educ*., **62**, 459 (1985).
[65] A. Brandt, J. Gräsvik, J. P. Hallett, T. Welton, *Green Chem*., **15**, 550 (2013).
[66] A. M. da Costa Lopes, K. G João, A. R. C. Morais, E. Bogel-Łukasik, R. Bogel-Łukasik, *Sus. Chem. Proc*., **1**, 3 (2013).